A Semi-Theoretical Study on the Effect of Rough Beds on the Conjugate Depth Ratio in Hydraulic Jumps

Khechiba Haroun
UDERZA Unit, Faculty of Technology, University of El Oued, 39000 El Oued, Algeria
khechiba-haroun@univ-eloued.dz (corresponding author)

Ali Ghomri
Research Laboratory in Underground and Surface Hydraulics, University of Biskra | Department of Hydraulics and Civil Engineering, University of El Oued, Algeria
alighomri@yahoo.fr

Djamel Besser
UDERZA Unit, Faculty of Technology, University of El Oued, 39000 El Oued, Algeria
djamel-besser@univ-eloued.dz

Ibtissam Herri
UDERZA Unit, Faculty of Technology, University of El Oued, 39000 El Oued, Algeria
herri-ibtissam@univ-eloued.dz

Received: 28 February 2025 | Revised: 25 March 2025 | Accepted: 4 April 2025

ABSTRACT

This study examines the effects of bed roughness on hydraulic jump characteristics in rectangular composite channels. Experiments were conducted in a laboratory flume with two roughness zones: the main channel and the floodplain, using uniform plastic granules to simulate different roughness conditions. The results show that increased bed roughness significantly reduces the subsequent depth ratio. A semi-theoretical dimensionless approach was developed to analyze the hydraulic jump, incorporating key parameters, such as the incident Froude number, the resistance coefficient, the expansion ratio, the shape factor, and the conjugate depth ratio. This approach, based on Euler's theory applied between two sections of the hydraulic jump, allows the conjugate depth ratio to be predicted using the flow rate and the tested absolute roughness values. The experimental validation confirms the accuracy of this model in estimating the conjugate depth ratio under varying roughness conditions. The developed approach provides a practical tool for engineers to optimize hydraulic structures in channels with variable roughness and zero slope, improving flow regulation and reducing erosive forces.

Keywords-hydraulic jump; bed roughness; conjugate depth ratio; rectangular compound channel; rough bed

I. INTRODUCTION

The hydraulic jump, a rapid transition from supercritical to subcritical flow, plays a critical role in energy dissipation and scour prevention in hydraulic structures [1, 2]. Classical theories have established fundamental relationships for jump characteristics in smooth rectangular channels [3], but real-world applications involving complex geometries and rough bed conditions require advanced analysis of turbulence dynamics and energy dissipation [4, 5]. Authors in [6, 7] show that rough beds enhance energy dissipation and reduce the subsequent depth ratios by altering turbulence structures. For example, corrugated or pebbled beds induce secondary flows, increase shear stresses, and stabilize jump positions [8, 9]. Submerged jumps over rough transition beds further reveal universal scaling laws for turbulence intensities [10, 11], highlighting the interaction between the roughness elements and flow regimes [12, 13]. Compound channels with distinct main and floodplain beds introduce additional complexity due to lateral variations in geometry and roughness. While authors in [14] examined hydraulic jumps in straight compound channels, authors in [15, 16] showed that roughened stilling basins reduce jump lengths by up to 40%. Research on triangular corrugated beds [17] emphasizes the role of bed orientation in flow separation, while compound roughness configurations in inclined channels alter the roll length and energy loss [18, 19]. However, these studies often overlook roughness interactions in multi-bed systems under zero-slope conditions, despite their prevalence in urban drainage networks [20]. Authors in [21, 22] examined the effects of roughness on bounce characteristics, confirming that bed texture significantly affects conjugate depth ratios and turbulence patterns in rectangular channels under varying flow conditions. The objective of this study was to develop a semi-theoretical mathematical model, a hybrid approach that integrates fundamental theoretical equations (e.g., Euler's equations or momentum conservation principles) with experimentally derived relationships, to analyze hydraulic jump dynamics in rectangular compound channels. The research began by applying Euler's equations between two cross-sections of a stabilized hydraulic jump, setting up dimensionless relationships between key parameters, such as incident Froude number (F_r), conjugate depth ratio (Y), resistance coefficient (C_r), channel expansion ratio (β), and shape factor (τ). Although the theoretical framework provided the foundation, critical unknowns such as C_r, which depends on channel roughness and flow conditions, were resolved empirically through laboratory experiments. A specialized test rig allowed comprehensive measurements under controlled conditions, with four uniformly distributed plastic roughness configurations (ε = 6, 8, 10, 12 mm) ensuring homogeneity, unlike previous studies using irregular surfaces [23, 24]. By explicitly correlating C_r with measurable roughness (ε), the model combined universal physical laws with site-specific empirical data, yielding highly accurate dimensionless equations for predicting Y using variables, such as flow rate and ε. This semi-theoretical approach differs from fully theoretical models (which rely solely on closed-form equations) and purely empirical models (which lack physical principles), and offers a robust tool for predicting hydraulic jump behavior in different flow scenarios, thereby advancing methods in mixed-channel hydraulics.

II. EXPERIMENTAL PROTOCOL

The study was conducted using a closed-loop hydraulic flume system at the Laboratory for Exploitation and Valorization of Natural Resources in Arid Zones, University of Ouargla, as shown in Figure 1. The primary test facility consisted of a 10-meter-long, horizontal (zero slope), rectangular composite channel with transparent plexiglas side walls for flow visualization. The channel was divided into a 4-meter experimental section with a compound cross-section consisting of a minor bed (14.4 cm wide) and a major bed (25 cm wide), both 15.5 cm high. A 150 mm diameter circular pipe supplied water from an axial pump (maximum capacity: 55.55 L/s) to an upstream closed metal box containing a flat orifice plate to induce a controlled torrential flow. The orifice's adjustable opening corresponded to the initial hydraulic head (h_1), which was controlled by a downstream sluice. A rectangular sharp-crested weir, installed at the channel's downstream end, enabled direct flow measurement. The experiments were conducted using four initial heights (h_1 =: 2.5 cm, 3 cm, 3.5 cm, and 4 cm), selected to achieve practical Froude number ranges ($F_r \approx 2 - 9$) relevant to real-world scenarios, like spillways and stilling basins, ensuring stable jump formation. The experiments were performed with four roughness values (ε = 06 mm, 08 mm, 10 mm, and 12 mm), chosen to reflect industrial and natural analogs (e.g., concrete channels and rock-bedded streams were utilized, with ε/B ratios maintaining flow homogeneity.

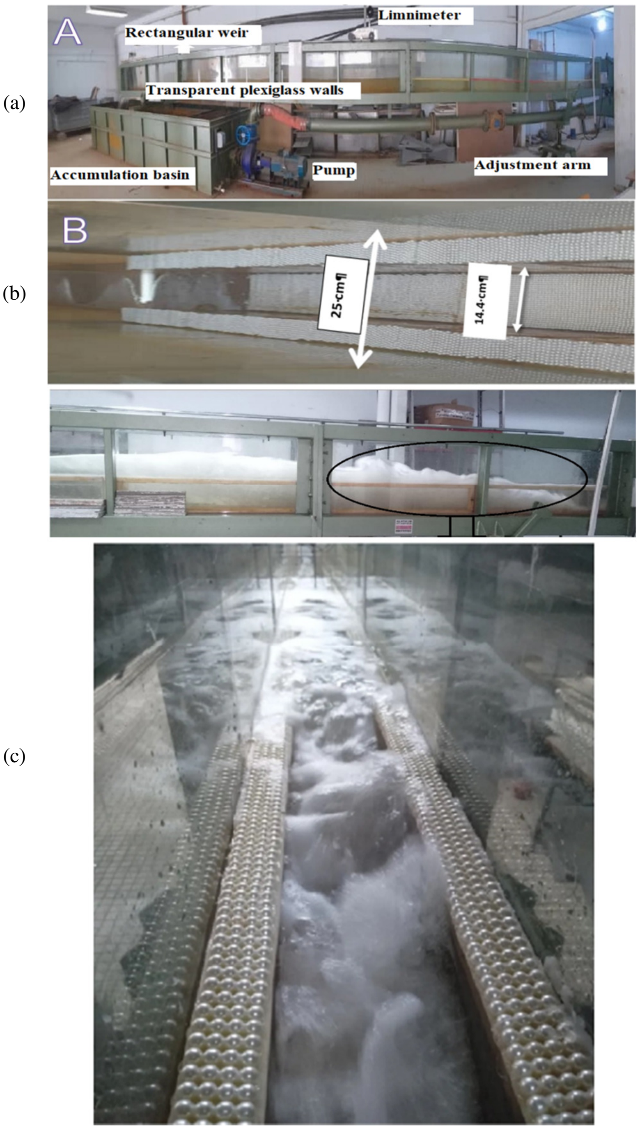

Fig. 1. (a) The experimental channel used for studying the hydraulic jump, (b) a cross-section of the compound channel showing the dimensions of the main bed and the secondary bed, (c) hydraulic jump formation in a rectangular compound channel with small and large rough beds.

Plastic pellets with a central hole were employed as roughness elements, securely attached with a rigid fishing line and arranged linearly along the channel bed. These elements were glued with a robust adhesive to prevent erosion and detachment during torrential flow, offering durability for multiple uses. Materials, like paper, glass, sheet metal, or gravel, were selected over for their rigidity and resistance to high-flow conditions, as presented in Figure 2. In addition, the study examined 26 adjustable thresholds (2.5 cm –21 cm) composed of thin metal plates (1 mm –2 mm thick) anchored to the channel bed in 1 cm increments. These thresholds were utilized to vary tailwater levels and cover subcritical to supercritical flow transitions. The influence of these thresholds on jump control was assessed. A schematic representation of the model is provided in Figure 3, including the channel layout, mat positions, and measurement points.

III. THEORETICAL ANALYSIS

The objective of this section is to establish a theoretical dependence governing the transition of the flow from the torrential (supercritical) regime to the fluvial (subcritical) regime in a rough compound channel, using Euler's theory. The desired dimensionless function is expressed as f (Y, F_r, C_r, β, τ) =0, where Y is the ratio of flow depths (h_2/h_1), F_r is the upstream Froude number, $\tau=h_1/h_c$ is the shape ratio, $\beta=b/B$ is the channel width expansion ratio, C_r is the resistance parameter accounting for roughness effects. The momentum balance between the initial (upstream) and final (downstream) sections of the hydraulic jump is:

$$\rho Q(v_1 - v_2) = F_1 - F_2 - F_r \quad (1)$$

where F_1 and F_2 are the hydrostatic forces at the upstream and downstream sections, and F_R is the friction force due to roughness, as depicted in Figure 4.

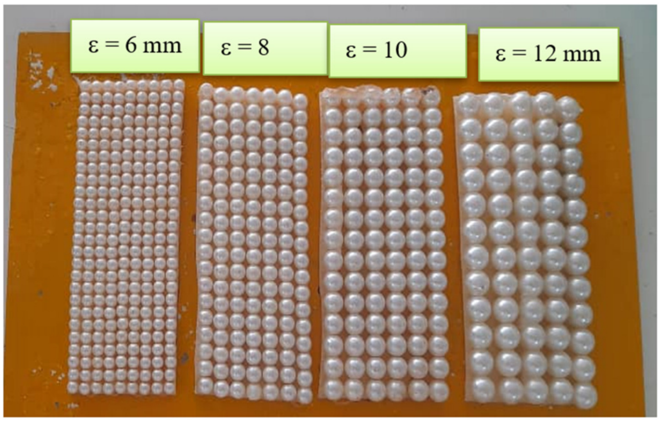

Fig. 2. Mats with varying roughness used in hydraulic jump experiments.

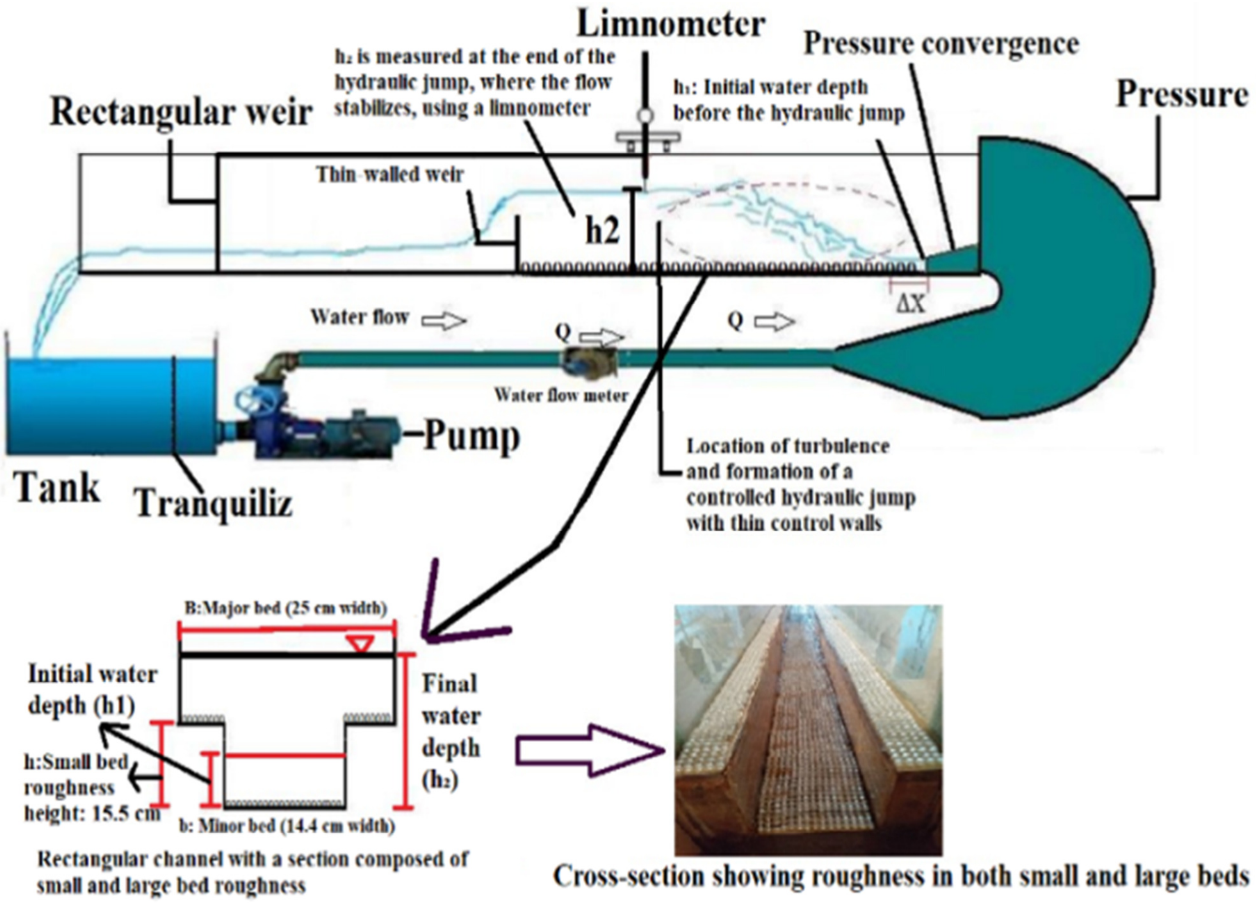

Fig. 3. Longitudinal section of the experimental model showing the channel layout, mat positions, and measurement points.

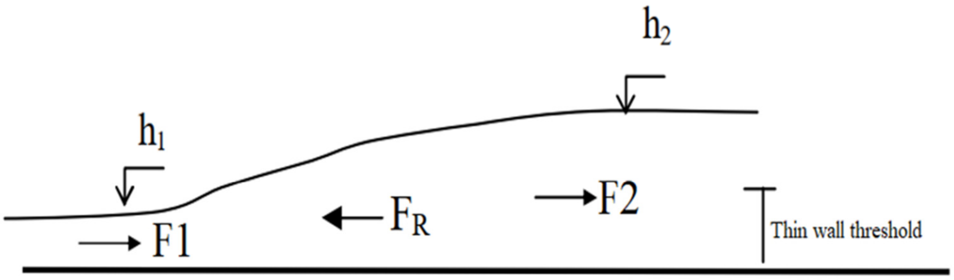

Fig. 4. Schematic representation of a hydraulic jump over a thin-wall threshold.

The initial and final sections are:

$$A_1 = bh_1 \quad (2)$$

$$A_2 = B(h_2 - h) + bh \quad (3)$$

The magnitude of hydrostatic forces is related to the water depth and channel width:

$$F_1 = \rho Q\left(\frac{h_1}{2}\right) bh_1 \quad (4)$$

$$F_2 = \rho Q(h_2 - h/2)bh + \rho Q[(h_2 - h)/2]B(h_2 - h) \quad (5)$$

where, h_1 and h_2 are the depths, b and B are the widths, ρ is water density, and g is the gravitational acceleration. Roughness resistance is:

$$F_r = C\rho gLj\left(\frac{V_1^2}{2g}\right)p \quad (6)$$

where C is the roughness coefficient, L_j is the jump length, $p=B$ is the wetted perimeter, and V is the flow velocity. The adjusted equation becomes:

$$\rho Q^2\left(\frac{1}{bh_1} - \frac{1}{B(h2-h)+bh}\right) = -\varpi\left(\frac{h_1}{2}\right)bh_1 + \varpi\left(h_2 - \frac{h}{2}\right)bh + \varpi\left[\frac{(h_2-h)}{2}\right]B(h_2 - h) \quad (7)$$

The final modified equation becomes:

$$F_r{}^2\left(1 - \frac{C_r}{\beta}\right) = \frac{-1+\frac{\left(2Y-\frac{1}{\tau}\right)}{\tau}+\frac{\left(Y-\frac{1}{\tau}\right)^2}{\beta}}{2} + \frac{\beta F_r{}^2}{Y-\frac{(1-\beta)}{\tau}} \quad (8)$$

where the incident Froude number is given by $\mathrm{F}_r = \frac{\mathrm{Q}}{\sqrt{\mathrm{b}^2\mathrm{h}_1^3\mathrm{g}}}$, while the channel expansion ratio is expressed as $\beta = \frac{\mathrm{b}}{\mathrm{B}}$, the conjugate depth ratio is $Y = \frac{h2}{h1}$, whereas the shape factor is defined as $\tau = \frac{h_1}{\mathrm{h}}$, and the friction coefficient is $C_r = \frac{Lj}{h1}$.

IV. EXPERIMENTAL STUDY OF THE SEMI-THEORETICAL RELATION

This section evaluates the friction coefficient C_r through laboratory experiments. The study's objective is to ascertain the variation of C_r with the Froude number (F_r) and surface roughness ε. The semi-theoretical relation is subjected to experimental testing and expressed by (8). To facilitate the experimental analysis, the expression $f(Y)$ is defined as:

$$f\,(Y) = F_r{}^2\left(1 - \frac{C_r}{\beta}\right) \quad (9)$$

Substituting this into (8):

$$f(Y) = \frac{-1+\frac{\left(2Y-\frac{1}{\tau}\right)}{\tau}+\frac{\left(Y-\frac{1}{\tau}\right)^2}{\beta}}{2} + \frac{\beta \mathrm{F_r}{}^2}{Y-\frac{(1-\beta)}{\tau}} \quad (10)$$

The variation of $f(Y)$ with F_r^2 is analyzed for four roughness values: ε = 06 mm, ε = 08 mm, ε = 10 mm, and ε = 12 mm. These values are different levels of bed roughness that affect the coefficient of friction C_r, as shown in Figure 5.

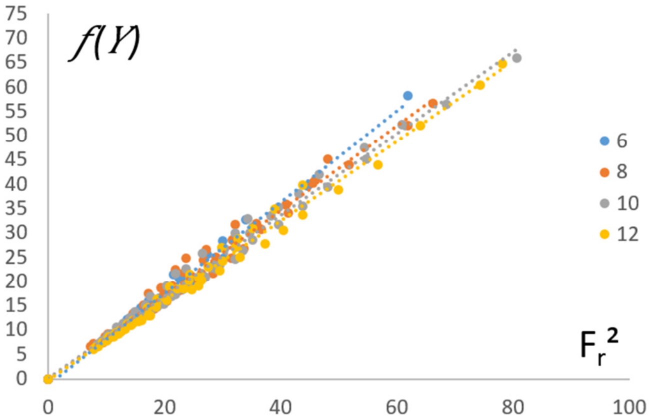

Fig. 5. Variation of $\mathrm{f}\,(\mathrm{Y}) = F_r{}^2\left(1 - \frac{C_r}{\beta}\right)$ as a function of Fr^2 with different bed roughness values.

A thorough examination of the experimental data collected from hydraulic jump measurements reveals that the distribution of data points for each pattern can be precisely represented by a linear relationship:

$$F_r{}^2T = \frac{-1+\frac{\left(2Y-\frac{1}{\tau}\right)}{\tau}+\frac{\left(Y-\frac{1}{\tau}\right)^2}{\beta}}{2} + \frac{\beta F_r{}^2}{Y-\frac{(1-\beta)}{\tau}} \quad (11)$$

where T is he factor $(1 - \frac{C_r}{\beta})$. A summary of the Cr coefficients is provided in Table I.

The data presented, suggest a positive correlation between the parameter C_r and the relative roughness (ε/B). A statistical correlation analysis of the paired values (ε/B, C_r) gives a linear relationship that can be expressed by: Cr = 0.4166 (ε/B), as portrayed in Figure 6. By substituting the expression for C_r into (11), the semi-theoretical equation is transformed as:

$$F_r{}^2\left(1-\frac{0.4166\left(\frac{\varepsilon}{B}\right)}{\beta}\right)=\frac{-1+\frac{\left(2Y-\frac{1}{\tau}\right)}{\tau}+\frac{\left(Y-\frac{1}{\tau}\right)^2}{\beta}}{2}+\frac{\beta F_r{}^2}{Y-\frac{(1-\beta)}{\tau}} \quad (12)$$

The curve in Figure 7 presents a strong relationship between $f(Y)$ and $F_r{}^2(1-\frac{0.4166\,(\varepsilon/B)}{\beta})$. The data points are distributed in a close pattern, suggesting a substantial degree of agreement between the experimental data and the theoretical predictions. This distribution confirms the accuracy and reliability of the measurements and shows that the actual values of $f(Y)$ agree well with the predicted values calculated using the given mathematical relationship.

TABLE I. THE VALUES OF THE CR

Roughness (mm)	Relative roughness (ε/B)	Parameter (C_r)	R^2
6	0.024	0.0688	0.9835
8	0.032	0.0792	0.9804
10	0.04	0.0924	0.9886
12	0.048	0.1095	0.9892
0 (smooth)	0	0	1

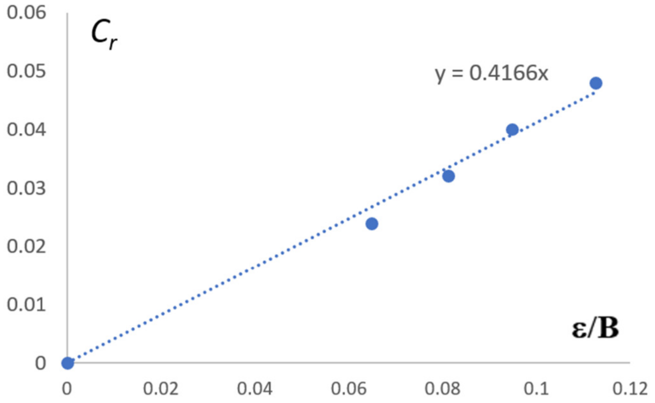

Fig. 6. Variation of C_r as a function of ε/B.

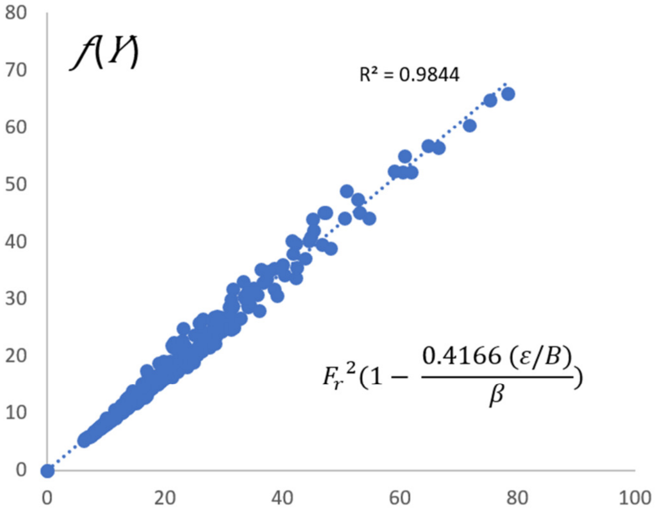

Fig. 7. Variation of $f(Y)$ with respect to $F_r{}^2(1-\frac{0.4166\,(\varepsilon/B)}{\beta})$.

The application of the Buckingham π theorem resulted in a general form $Y=aF_r{}^m(1-\frac{0.4166\,(\varepsilon/B)}{\beta})^n$, displayed in Figure 8. The unknown coefficients (a, m, n) were determined through nonlinear regression using experimental measurements. The least squares method was then employed to optimize these parameters:

$$Y=1.329F_r^{0.986}(1-\frac{0.4166\,(\varepsilon/B)}{\beta})^{1.430} \quad (13)$$

The graph shown in Figure 9 demonstrates the relationship between the experimental values ($Y_{\text{Experimental}}$) and a mathematical model based on an empirical equation. The data points exhibit a high degree of alignment with the trend line, suggesting a strong correlation between the predicted and experimental values.

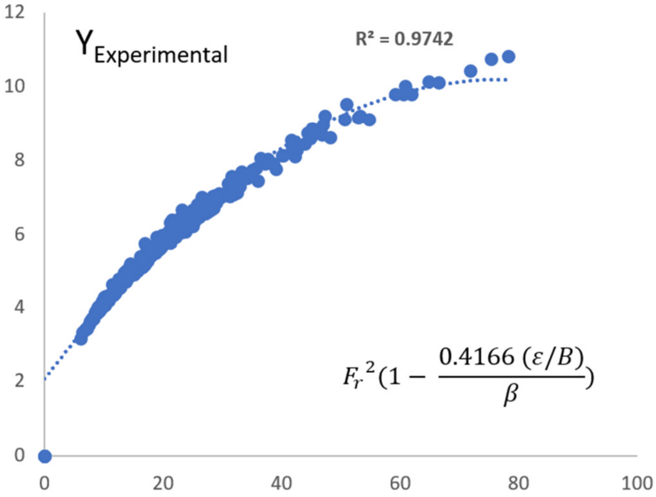

Fig. 8. Variation of $Y_{Experimental}$ with respect to $F_r{}^2(1-\frac{0.4166\,(\varepsilon/B)}{\beta})$.

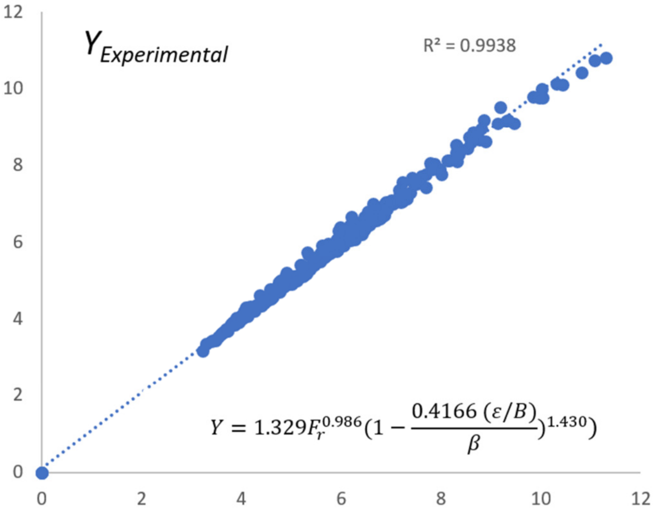

Fig. 9. Variation of $Y_{Experimental}$ with respect to $Y=1.329F_r^{0.986}\left(1-\frac{0.4166\left(\frac{\varepsilon}{B}\right)}{\beta}\right)^{1.430}$.

V. CONCLUSIONS

This study shows that bed roughness significantly influences hydraulic jump characteristics in rectangular compound channels. The experimental results reveal that increasing roughness reduces the sequent depth ratio, following the empirical trend $Y = 1.329F_{\mathrm{r}}^{0.986}(1 - \frac{0.4166\ (\varepsilon/\mathrm{B})}{\beta})^{1.430}$, indicating that the sequent depth ratio (Y) decreases as the friction coefficient C_r increases. A semi-theoretical, dimensionless model was developed based on Euler's equations applied between two sections of the hydraulic jump. The model incorporates key hydraulic parameters, including the incident Froude number, resistance coefficient, expansion ratio, and absolute roughness. This enables an accurate prediction of the conjugate depth ratio. The experimental validation confirms that the model reliably captures the effects of roughness variations on hydraulic jump behavior. The findings offer a pragmatic approach for optimizing hydraulic structures, particularly in energy dissipation systems, flood control channels, and stilling basins, underscoring the significance of roughness design in stabilizing hydraulic jumps and mitigating structural erosion.

ACKNOWLEDGMENT

The authors would like to express their deep gratitude and appreciation for the support and contributions of the Renewable Energy Development Unit in Arid Zones (UDERZA), which played a pivotal role in providing the research environment and necessary resources for the completion of this work.

REFERENCES

[1] W. H. Hager, *Energy Dissipators and Hydraulic Jump*,. Dordrecht, Netherlands: Springer Netherlands, 1992.

[2] N. Rajaratnam, "Hydraulic Jumps," in *Advances in Hydroscience*, vol. 4, V. T. Chow, Ed. Elsevier, 1967, pp. 197–280.

[3] F. G. Carollo, V. Ferro, and V. Pampalone, "Hydraulic Jumps on Rough Beds," *Journal of Hydraulic Engineering*, vol. 133, no. 9, pp. 989–999, Sep. 2007, https://doi.org/10.1061/(ASCE)0733-9429(2007)133:9(989).

[4] S. Dey and A. Sarkar, "Characteristics of Turbulent Flow in Submerged Jumps on Rough Beds," *Journal of Engineering Mechanics*, vol. 134, no. 1, pp. 49–59, Jan. 2008, https://doi.org/10.1061/(ASCE)0733-9399(2008)134:1(49).

[5] H. J. Leutheusser and E. W. Schiller, "Hydraulic jump in open channels—some properties," *Journal of Hydraulic Research*, vol. 13, no. 1, pp. 17–36, 1975.

[6] H. Velioğlu, "Effect of rough bed on hydraulic jump characteristics," *Water Science and Engineering*, vol. 5, no. 1, pp. 95–106, 2012.

[7] S. A. Ead and N. Rajaratnam, "Hydraulic Jumps on Corrugated Beds," *Journal of Hydraulic Engineering*, vol. 128, no. 7, pp. 656–663, Jul. 2002, https://doi.org/10.1061/(ASCE)0733-9429(2002)128:7(656).

[8] F. Bahmanpouri, C. Gualtieri, and H. Chanson, "Flow patterns and free-surface dynamics in hydraulic jump on pebbled rough bed," *Proceedings of the Institution of Civil Engineers - Water Management*, vol. 176, no. 1, pp. 32–49, Apr. 2021, https://doi.org/10.1680/jwama.20.00040.

[9] N. Afzal, A. Bushra, and A. Seena, "Analysis of Turbulent Hydraulic Jump over a Transitional Rough Bed of a Rectangular Channel: Universal Relations," *Journal of Engineering Mechanics*, vol. 137, no. 12, pp. 835–845, Dec. 2011, https://doi.org/10.1061/(ASCE)EM.1943-7889.0000294.

[10] U. Türker and M. Valyrakis, "Hydraulic jump on rough beds: conceptual modeling and experimental validation," *Water Supply*, vol. 21, no. 4, pp. 1423–1437, Nov. 2020, https://doi.org/10.2166/ws.2020.292.

[11] N. Agrawal and E. Padhi, "Impacts of bed roughness and orientation on hydraulic jump: A review," *Water Science and Engineering*, vol. 18, no. 1, pp. 90–101, Mar. 2025, https://doi.org/10.1016/j.wse.2024.03.003.

[12] L. A. M. Saleh and S. I. Khassaf, "A review study on the effect of artificial bed roughness on the performance of prismatic hydraulic jump stilling basins," *AIP Conference Proceedings*, vol. 3091, no. 1, May 2024, Art. no. 020010, https://doi.org/10.1063/5.0205769.

[13] A. Benabdesselam, B. Achour, and L. Houichi, "Hydraulic Jumps in a Straight Rectangular Compound Channel: Theoretical Approach and Experimental Study," *LARHYSS Journal*, vol. 29, pp. 323–340, Jan. 2017.

[14] T. Mohamed Ali, "Effect of roughened-bed stilling basins on the characteristics of hydraulic jumps," *Journal of Hydraulic Research*, vol. 29, no. 5, pp. 565–585, 1991.

[15] R. Maleki and V. Fiorotto, "Experimental investigation of hydraulic jumps over roughened beds in rectangular channels," *Journal of Hydraulic Engineering*, vol. 147, no. 8, Aug. 2021, https://doi.org/10.1061/(ASCE)HY.1943-7900.0001926.

[16] H. Samadi-Boroujeni, M. Ghazali, B. Gorbani, and R. F. Nafchi, "Effect of triangular corrugated beds on the hydraulic jump characteristics," *Canadian Journal of Civil Engineering*, vol. 40, no. 9, pp. 841–847, Sep. 2013, https://doi.org/10.1139/cjce-2012-0019.

[17] M. K. Beirami and M. R. Chamani, "Hydraulic jump in sloping channels: roller length and energy loss," *Canadian Journal of Civil Engineering*, vol. 37, no. 4, pp. 535–543, Apr. 2010, https://doi.org/10.1139/L09-175.

[18] M. Kumar and A. S. and Lodhi, "Hydraulic jump over sloping rough floors," *ISH Journal of Hydraulic Engineering*, vol. 22, no. 2, pp. 127–134, May 2016, https://doi.org/10.1080/09715010.2015.1088409.

[19] A. Kavousizadeh, S. Eslamian, and V. P. Singh, "Analysis of hydraulic jump on rough beds in urban drainage systems," *Urban Water Journal*, vol. 16, no. 2, pp. 121–131, 2019.

[20] S. K. Gupta and V. K. Dwivedi, "Experimental investigation of hydraulic jump characteristics in sloping rough surfaces for sustainable development," *Engineering Research Express*, vol. 6, no. 2, Apr. 2024, Art. no. 025103, https://doi.org/10.1088/2631-8695/ad3acf.

[21] N. M. Ngoc and T. N. Thang, "A Study of an Empirical Sequent Depths Equation of the Hydraulic Jump in a Horizontal Trapezoidal Channel," *Engineering, Technology & Applied Science Research*, vol. 13, no. 6, pp. 12307–12313, Dec. 2023, https://doi.org/10.48084/etasr.6431.

[22] D. Valero, N. Viti, and C. Gualtieri, "Numerical Simulation of Hydraulic Jumps. Part 1: Experimental Data for Modelling Performance Assessment," *Water*, vol. 11, no. 1, Jan. 2019, Art. no. 36, https://doi.org/10.3390/w11010036.

[23] A. Ghomri and F. Riguet, "Le ressaut hydraulique dans les canaux prismatique à parois rugueuses," Ph.D. dissertation, Université Mohamed Khider-Biskra, Biskra, Algeria, 2012.

[24] M. Debabeche, S. Kateb, and A. Ghomri, "Étude expérimentale du ressaut hydraulique dans un canal triangulaire à parois rugueuses," *LARHYSS Journal*, vol. 4, no. 1, pp. 187–196, Jun. 2006.